Quadrupole interaction of ^{125}Te and ^{129}I in polycrystalline Te and in Te single crystals

G. Langouche,* M. Van Rossum, K. P. Schmidt, and R. Coussement
Instituut voor Kern-en Stralingsfysika, Universiteit te Leuven, Belgium
(Received 10 August 1973)

An investigation was performed about the ion implantation of radioactive nuclei into Te single crystals. Although ^{125m}Te was implanted to a relatively high dose, the Mössbauer spectra of these sources indicate a substitutional implantation and a maintainance of the single-crystal lattice. Using ^{129m}Te sources in a polycrystalline Te lattice and a CuI absorber, $e^2qQ = -404 \pm 4$ MHz, $\eta = 0.73 \pm 0.02$, and $\delta = -1.19 \pm 0.04$ mm/sec were measured. Using ^{129m}Te sources implanted in a Te single crystal, the angle between the crystal c axis and the z axis of the electric field gradient was measured to be less than 15°. In all these experiments no definite evidence for the Goldanskii-Karyagin effect in the Te lattice was found.

I. INTRODUCTION

Single crystals with a large electric field gradient (EFG) at the site of the radioactive nucleus can be used in nuclear-orientation experiments at low temperatures, or in perturbed-angular-correlation experiments, to measure quadrupole moments of excited nuclear states. However, not only the magnitude (V_{zz}) and the asymmetry parameter η [$\eta = (V_{xx} - V_{yy})/V_{zz}$] of the EFG must be known, but also the orientation of the principal-axis system (PAS) relative to the crystal set of axes. Another difficulty which arises is the fact that the radioactive atoms have to be built into the single crystal, and that one must be sure that they occupy regular lattice sites.

Mössbauer spectroscopy can give a solution to both problems. The EFG-tensor parameters can be measured using single-crystal sources or absorbers. The Mössbauer spectra of sources, built into single crystals, indicate whether the nucleus is subjected to the right hyperfine interaction. For these experiments we are restricted, of course, to Mössbauer nuclei, but the results concerning the EFG and the quality of the sources can be extended to all isotopes of the same element.

In the present work we made an investigation about the use of Te single crystals as hosts for Te and I sources. The EFG of Te in Te has been studied extensively[1,2] by several groups by Mössbauer spectroscopy on ^{125}Te, using Te single crystals as absorbers. So we were able to test the quality of sources made by ion implantation of ^{125m}Te by an isotope separator into Te single crystals, by taking Mössbauer spectra of these sources, using a single-line ^{125}Te absorber, and by comparing them with the known spectra. Once the quality was tested, sources were made by implantation of ^{129m}Te into Te single crystals, and Mössbauer spectra of ^{129}I were recorded. As the orientation of the PAS of I in Te was still unknown, these spectra gave us the opportunity to measure the remaining parameters of the EFG tensor, so that the Te single crystals can also be used to study quadrupole moments of I nuclear states.

II. EXPERIMENTAL PROCEDURE

The ^{125m}Te and ^{129m}Te activity was obtained by irradiating enriched ^{124}Te and ^{128}Te samples at a flux of about 3×10^{14} n/cm^2 sec at the BR2 reactor in Mol, Belgium for about six weeks.

The single crystals were cut from a Te single-crystal bar into slices of about 1-mm thickness and about 13-mm diam using a chemical saw with Honeywell etching fluid.[3] This procedure is necessary to avoid damage of the single-crystal surface.

The implantation into the single crystal was done with the Leuven Isotope Separator in our institute, at an accelerating voltage of about 75 kV. The activities obtained in this way were typically of the order of 20–30 μCi. The implantation doses were of the order of 5×10^{15} atoms/cm^2 for the ^{125m}Te source (due to the presence of some ^{125}Te in the enriched ^{124}Te sample), and of the order of 5×10^{14} atoms/cm^2 for ^{129m}Te.

The absorbers used for these experiments were a ZnTe absorber, containing 2-mg/cm^2 ^{125}Te, and a CuI absorber containing 10-mg/cm^2 ^{129}I. As ^{129}I itself decays to ^{129}Xe, giving Xe x rays, a thin indium foil was placed right behind the CuI absorber to absorb these x rays preferentially.

The ^{125}Te spectra were recorded using a 0.2-mm-thick NaI (Tl) scintillator, and detecting the escape peak of the 35-keV radiation. On the other hand, a 3-mm-thick NaI (Tl) scintillator was used for the detection of the 27.7-keV radiation in ^{129}I. The scintillators were attached to a low-noise EMI 9514 SA photomultiplier.

In the cryostat used in this experiment, both source and absorber were held at the same temperature. All single-crystal measurements were done at liquid-helium temperature. The source

was moved by a drive system of the Kankeleit type in the constant-acceleration mode, and a calibration spectrum was recorded simultaneously.

III. LINE POSITIONS AND INTENSITIES

In the PAS of the EFG, the quadrupole interaction Hamiltonian is given by[4]

$$H=\frac{e^2qQ}{4I(2I-1)}\left(3\hat{I}_z^2-\hat{I}^2+\frac{\eta}{2}(\hat{I}_+^2+\hat{I}_-^2)\right) \quad (1)$$

(operators are characterized by a caret). Here Q stands for the nuclear quadrupole moment and $eq=V_{zz}$ for the largest component of the EFG in its diagonal form. In order to calculate Mössbauer line positions, the secular equations[5] obtained by the diagonalization of the energy matrix have to be used. For ^{125}Te a $I=\frac{3}{2}\rightarrow I=\frac{1}{2}$ transition occurs, and only the excited level is split, giving rise to the well-known quadrupole doublet. For ^{129}I a $I=\frac{5}{2}\rightarrow I=\frac{7}{2}$ transition occurs, and 12 Mössbauer line positions can be calculated. We used the experimental ratio $Q_e/Q_g=1.23\pm0.02$,[6] and we calculated the peak positions in units of e^2qQ_g. The result is shown in Fig. 1 as a function of η. The meaning of the transition numbers is shown in Table I. It is obvious from this figure that the positions of the Mössbauer peaks alone give enough evidence to determine the value of V_{zz} and η of the EFG. The value of η only depends on the relative distances between the Mössbauer peaks, while the V_{zz} value only depends on the absolute value of the splitting. Especially transitions 4, 5, 8, 9, 10, and 11 show a large η dependence. Their intensities, however, are not always large enough to be useful, as will be demonstrated below.

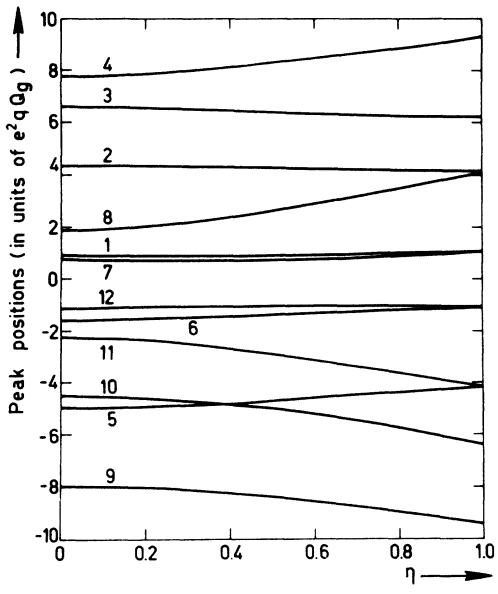

FIG. 1. Peak positions in the ^{129}I quadrupole-split Mössbauer spectrum.

TABLE I. Mössbauer transitions in the ^{129}I spectrum.

Transition number	Corresponding transition for $\eta=0$
1	$m=\pm\frac{5}{2}\rightarrow m=\pm\frac{7}{2}$
2	$m=\pm\frac{5}{2}\rightarrow m=\pm\frac{5}{2}$
3	$m=\pm\frac{5}{2}\rightarrow m=\pm\frac{3}{2}$
4	$m=\pm\frac{5}{2}\rightarrow m=\pm\frac{1}{2}$
5	$m=\pm\frac{3}{2}\rightarrow m=\pm\frac{7}{2}$
6	$m=\pm\frac{3}{2}\rightarrow m=\pm\frac{5}{2}$
7	$m=\pm\frac{3}{2}\rightarrow m=\pm\frac{3}{2}$
8	$m=\pm\frac{3}{2}\rightarrow m=\pm\frac{1}{2}$
9	$m=\pm\frac{1}{2}\rightarrow m=\pm\frac{7}{2}$
10	$m=\pm\frac{1}{2}\rightarrow m=\pm\frac{5}{2}$
11	$m=\pm\frac{1}{2}\rightarrow m=\pm\frac{3}{2}$
12	$m=\pm\frac{1}{2}\rightarrow m=\pm\frac{1}{2}$

For the transition probabilities between energy levels which cannot be characterized by a single magnetic quantum number, a general formula has been derived by Karyagin.[7] He defines b_M coefficients for a $I_e\rightarrow I_g$ transition:

$$b_M=\sum_{m_e m_g}(-1)^{m_g}\langle m_g|E_g\rangle^*\langle m_e|E_e\rangle \times\begin{pmatrix} I_g & l & I_e \\ m_g & M & -m_e\end{pmatrix}, \quad (2)$$

l being the multipolarity of the transition and $M=m_e-m_g$. The transition probability of a $M1$ transition ($l=1$ and $M=0,\pm1$) between an excited state $|E_e\rangle$ and a ground state $|E_g\rangle$ is then given by

$$P(|E_e\rangle\rightarrow|E_g\rangle)=(|b_{+1}|^2+|b_{-1}|^2)(1+\cos^2\theta)/2 +|b_0|^2\sin^2\theta+b_{+1}^*b_{-1}\sin^2\theta\cos2\phi. \quad (3)$$

The angles θ and ϕ describe the γ-ray direction in the PAS of the EFG. This angular distribution is not axially symmetric, due to the last interference term. This is due to $\eta\neq0$, as m_e and m_g then are not good quantum numbers and for one definite transition b_{+1} and b_{-1} can be different from zero simultaneously, giving rise to a nonaxial distribution pattern. For polycrystalline samples we integrate Eq. (3) over all angles, with the result

$$P(|E_e\rangle\rightarrow|E_g\rangle)=|b_{+1}|^2+|b_{-1}|^2+|b_0|^2. \quad (4)$$

As the energy levels are degenerate, four transition probabilities $P(|E_e\rangle\rightarrow|E_g\rangle)$ have to be summed to obtain the total transition probability $P_k(E_e\rightarrow E_g)$ between two energy levels, where k stands for

the transition number.

The transition probability can be worked out analytically for the $I=\frac{3}{2}\rightarrow I=\frac{1}{2}$ transition of ^{125}Te, and the resulting intensity ratio for the two peaks is given by[8]

$$\frac{P_1}{P_2}=\frac{4(1+\frac{1}{3}\eta^2)^{1/2}-(1-3\cos^2\theta-\eta\sin^2\theta\cos2\phi)}{4(1+\frac{1}{3}\eta^2)^{1/2}+(1-3\cos^2\theta-\eta\sin^2\theta\cos2\phi)}. \quad (5)$$

For $\eta=0$ transition 1 corresponds to the $\pm\frac{3}{2}\rightarrow\pm\frac{1}{2}$ transition, and transition 2 to the $\pm\frac{1}{2}\rightarrow\pm\frac{1}{2}$ transition. For polycrystalline samples we integrate Eq. (5) for all angles, with the result $P_1/P_2=1$.

For the $I=\frac{5}{2}\rightarrow I=\frac{7}{2}$ transition in ^{129}I we calculated all transition probabilities for polycrystalline samples as a function of η. The result is shown in Fig. 2. It is interesting to note that transitions 4, 5, 9, and 10, which are forbidden if $\eta=0$, become different from zero for $\eta\neq0$, due to the admixing of the m states. The largest η dependence of the relative intensities is to be seen for transitions 6, 7, 8, 11 and 20. However, as can be seen in Fig. 1, transitions 1 and 7, and also transitions 6 and 12, are very near to each other, and their components are experimentally resolved only for very large V_{zz}. The resulting composite peaks have an intensity ratio almost independent of η.

IV. POLYCRYSTALLINE SOURCES

Spectra were recorded using ^{125m}Te in its polycrystalline Te environment at temperatures of liquid nitrogen and liquid helium (Fig. 3). The measured quadrupole splittings were, respectively, 7.25 ± 0.08 and 7.74 ± 0.07 mm/sec, in good agreement with previous values.[1,9] The temperature dependence was already explained.[9] The mean isomer shift was $\delta=-0.66\pm0.04$ mm/sec.

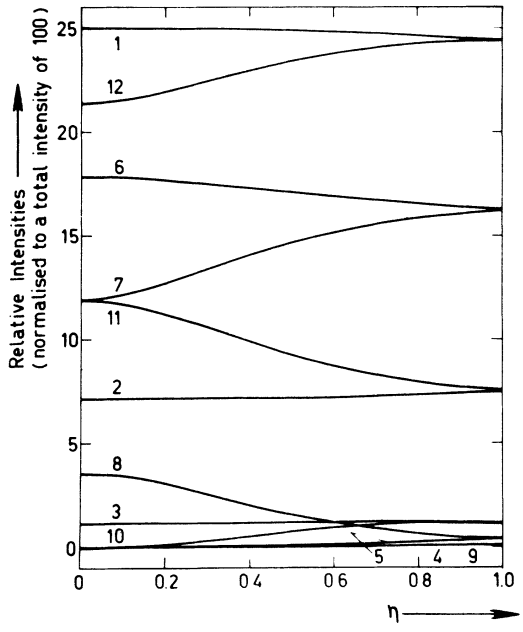

FIG. 2. Relative intensities in a $I=\frac{5}{2}\rightarrow I=\frac{7}{2}$ quadrupole-split spectrum.

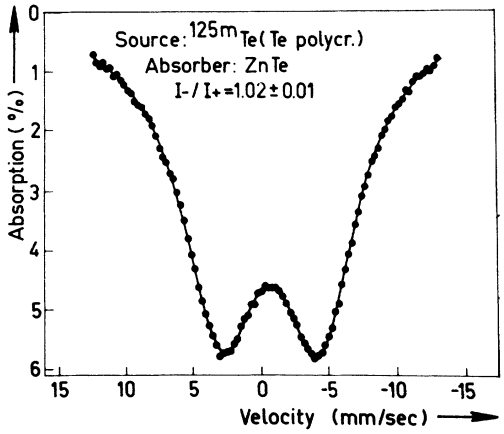

FIG. 3. Mössbauer spectrum of ^{125}Te in polycrystalline Te at liquid-He temperature.

We denote the intensity of the measured Mössbauer lines by I_+ for the line having a more positive velocity and by I_- for the line having a more negative velocity. As we are using a split source, I_+ corresponds to the least energetic transition and I_- to the most energetic transition in the source. This intensity ratio was fitted carefully for the spectrum at liquid-helium temperature (Fig. 3) and was found to be 1.02 ± 0.01. The question whether this asymmetry is due to the Goldanskii-Karyagin effect, or to a small texture in the powder source remains open. Similar spectra have been recorded by several authors[1,2,9] and, although most of them have seen an asymmetry which they ascribe to the Goldanskii-Karyagin effect, our asymmetries and theirs vary in magnitude and even in sign.

Also ^{129m}Te sources in a polycrystalline Te environment were measured at liquid-nitrogen and liquid-helium temperatures. The spectrum at liquid-helium temperature is shown in Fig. 4. The quadrupole splittings obtained at both temperatures were consistent with each other. We therefore adopt the mean values $e^2qQ=-404\pm4$ MHz, $\eta=0.73\pm0.02$, and $\delta=-1.19\pm0.04$ mm/sec. The fitting procedure described in Ref. 10 was used. The quadrupole splitting obtained by us is somewhat larger than other values reported before[11,12] (see Table II). We therefore tested our velocity calibration system, which consists of a second source at the opposite end of the driving rod, whose spectrum is recorded at the same time as the actual experiment. Using the same kind of source and

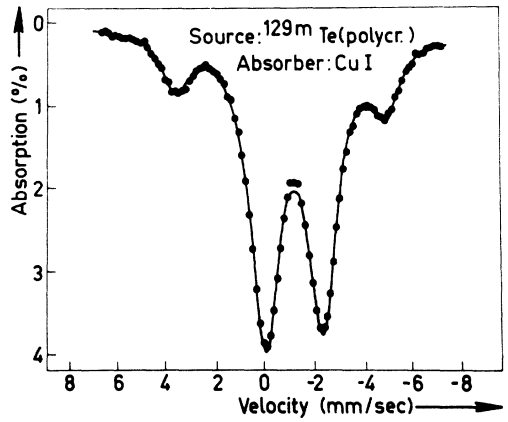

FIG. 4. Mössbauer spectrum of ^{129}I in polycrystalline Te at liquid-He temperature.

absorber at both ends, no discrepancies were found.

In the Mössbauer spectrum of ^{129}I in polycrystalline Te, the measured intensity ratios deviate somewhat from the theoretical ones. This can be explained by the Goldanskii-Karyagin effect, or by a small texture in the source.

V. SINGLE-CRYSTAL SAMPLES

The Te lattice is shown in Fig. 5(a). It consists of parallel spiral turns of Te atoms, which form a hexagonal network. Each spiral turn then contains three Te atoms, which have exactly the same surroundings as the preceding Te atom, if we rotate 120° around the spiral axis (c axis). This means that the Te lattice contains three equivalent positions, for which the EFG has the same magnitude V_{zz} and asymmetry η, but a different orientation of the PAS. We denote now by $(\alpha_i, \beta_i, \gamma_i)$ the Euler angles which define the orientation of these PAS with respect to the crystal set of axes (a, b, c). According to the symmetry just described, we have then

$$\alpha_1 = \alpha, \quad \alpha_2 = \alpha + 120°, \quad \alpha_3 = \alpha + 240°;$$

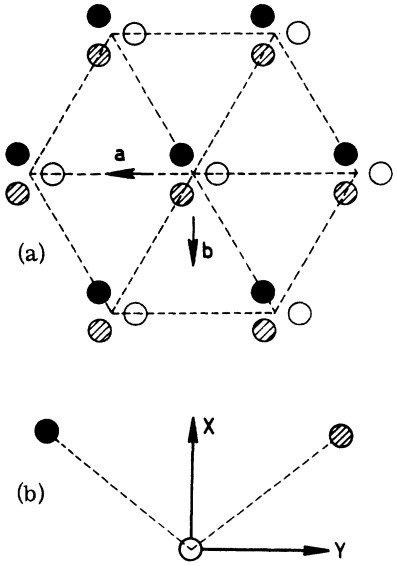

FIG. 5. (a) Te lattice. The empty circles represent Te sites in the plane of the paper ($\perp$ c axis). The other sites are in planes, respectively, at a distance $\frac{1}{3}c$ above and $\frac{1}{3}c$ under the first plane. The spiral structure is obvious. The lattice parameters are $c = 5.95$ and $a = 4.45$ Å. (b) Orientation of the PAS for Te in Te. The Te-Te-Te bond angle is 101.5°.

$$\beta_1 = \beta_2 = \beta_3 = \beta, \tag{6}$$

$$\gamma_1 = \gamma_2 = \gamma_3 = \gamma.$$

The angle β is the angle between the c axis and the PAS z axis. In a Mössbauer experiment one observes the sum of the contributions due to the three sites. Therefore we have to sum the expressions $P_k(\theta_i, \phi_i)$ obtained from Eq. (3) for the three lattice sites. At the same time it is convenient to transform the $P_k(\theta_i, \phi_i)$ expressions which depend on the angles θ_i and ϕ_i to the (a, b, c) axis system with the angles Θ and Φ (Fig. 6). The factors which have to be summed and transformed in Eq. (3) are $\cos^2\theta_i$ and $\sin^2\theta_i \cos 2\phi_i$. We performed the calculation in the Appendix, with the result

$$a \equiv \sum_{i=1,3} \cos^2\theta_i = \tfrac{3}{2}\sin^2\Theta \sin^2\beta + 3\cos^2\Theta \cos^2\beta,$$

TABLE II. Experimental values of e^2qQ, η, and the isomer shift for ^{129}I in Te.

Authors	Temperature (°K)	e^2qQ [a] (MHz)	η	δ [b] (mm/sec)
Pasternak *et al.* [c]	80	-373 ± 6	0.80 ± 0.05	-1.15 ± 0.05
Warren *et al.* [d]	80	-349 ± 11	0.69 ± 0.03	-0.94 ± 0.03
This work	4	-403 ± 4	0.73 ± 0.02	-1.19 ± 0.03
This work	80	-406 ± 6	0.73 ± 0.02	-1.18 ± 0.04

[a] The quadrupole moment used is the ground-state quadrupole moment of ^{129}I.
[b] The isomer shift is given for the ^{129}I in Te source relative to the CuI absorber.
[c] Reference 11.
[d] Reference 12.

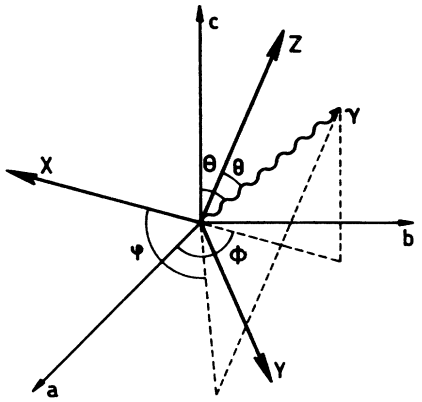

FIG. 6. γ-ray direction in the PAS and in the (a, b, c)-axis system.

$$b \equiv \sum_{i=1,3} \sin^2\theta_i \cos 2\phi_i \qquad (7)$$

$$= (\tfrac{3}{2}\sin^2\Theta \sin^2\beta - 3\cos^2\Theta \sin^2\beta)\cos 2\gamma.$$

We immediately note that these factors, and thus the intensity distributions of the Mössbauer peaks, are independent of the Euler angle α and of the measurement angle Φ. We remember that to obtain this important result we only used the fact that there are three equivalent sites in the Te lattice, which only differ by a rotation of 120° around the c axis. This explains the same intensity ratio measured[1,2] for the $[10\bar{1}0]$ and $[2\bar{1}\bar{1}0]$ directions.

In order to obtain the intensity ratio in a ^{125}Te single-crystal spectrum, Eq. (5) has to be summed for the three lattice locations, using Eqs. (7). The result is

$$\frac{I_1}{I_2} = \frac{\sum_{i=1,3} P_1(\theta_i, \phi_i)}{\sum_{i=1,3} P_2(\theta_i, \phi_i)}$$

$$= \frac{4[\frac{1}{3}(3+\eta^2)]^{1/2} - (1 - a - \frac{1}{3}\eta b)}{4[\frac{1}{3}(3+\eta^2)]^{1/2} + (1 - a - \frac{1}{3}\eta b)}, \qquad (8)$$

with a and b defined in Eqs. (7). From the known crystal structure of Te [Fig. 5(a)] and the known PAS orientation [Fig. 5(b)] the values $\beta = 62.5°$ and $\gamma = 0°$ can be deduced. The asymmetry parameter has been measured to be $\eta = 0.64 \pm 0.04$.[1] We use these values in Eq. (8) and obtain

γ ray parallel to c axis $I_1/I_2 = 0.66$,

γ ray perpendicular to c axis $I_1/I_2 = 1.23$.

Spectra were recorded for these γ-ray directions, and the results are shown in Figs. 7(a) and 7(b). We immediately identify transition I_1 with I_- and transition I_2 with I_+. This means that the quadrupole splitting e^2qQ is positive. This is in agreement with Ref. 1 but not with Ref. 2.

The measured asymmetries are somewhat weaker than the values given above. This is mostly due to the finite solid angle used in the experiment. A smaller η value gives also a small weakening of the asymmetry. The Te-Te-Te bond angle [Fig. 5(b)] has recently been measured to be 101.5° at the temperature of liquid He,[13] and, as the relation $\eta = |3\cos\theta|$ holds for this type of bonding,[14] a theoretical value $\eta = 0.60$ results, which thus could weaken the asymmetries given above to a small degree.

Also ^{129}I-spectra line intensities were calculated. A similar summation was performed, and the resulting intensities depend on η, Θ, β, and γ only. We made some computer simulations of ^{129}I spectra in Te single crystals using different values for β and γ and taking $\eta = 0.73$, as measured for the polycrystalline samples. The two deepest peaks of the spectrum, having several components, remain almost constant. The two side peaks, however, being transitions 2 and 11 show a clear β and γ dependence.

The experimental ^{129}I spectrum for the γ ray parallel to the c axis [Fig. 8(a)], shows a disappearance of peak 2. The best fit of this spectrum was obtained for $\beta = 0°$, and was independent of the value of γ. This is clearly shown in Fig. 9, where

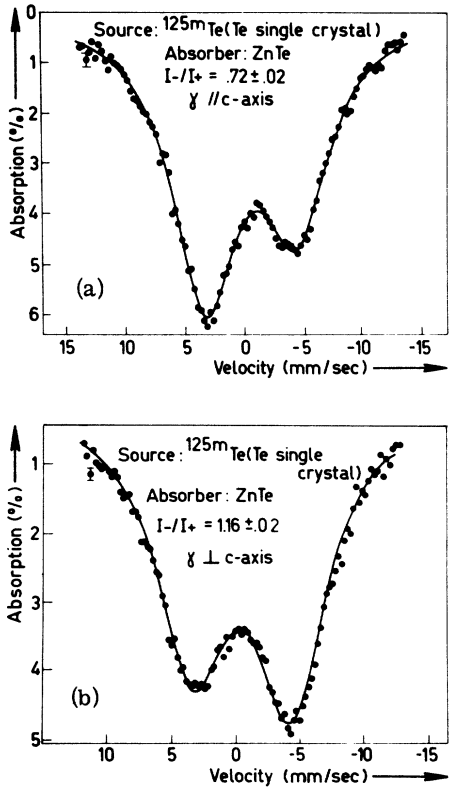

FIG. 7. Mössbauer spectra of ^{125}Te in a Te single crystal. (a) γ ray $\parallel$ c axis. (b) γ ray $\perp$ c axis.

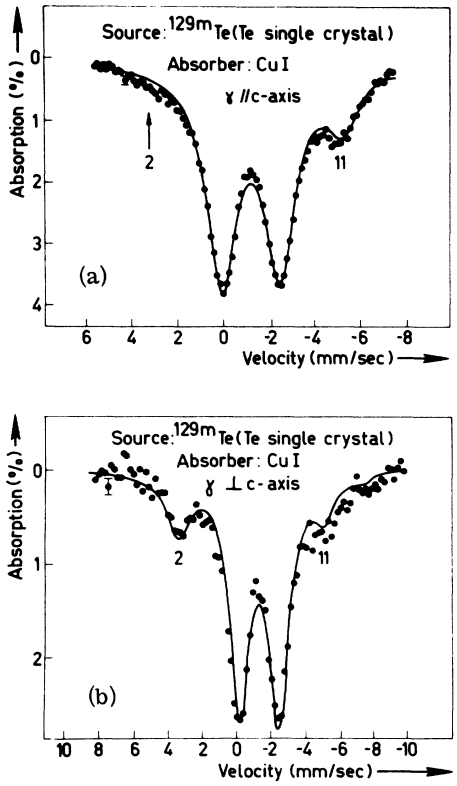

FIG. 8. Mössbauer spectra of ^{129}I in a Te single crystal. (a) γ ray $\parallel$ c axis. (b) γ ray $\perp$ c axis. As explained in the text, the solid line is not a best fit to the data.

the experimental and theoretical intensity ratios I_2/I_{11} are only consistent for a value of β smaller than 15°, which clearly cannot give any evidence about the value of γ. For the γ ray perpendicular to the c axis the theoretical β and γ dependence is not so explicit. The experimental spectrum also suffers from an insufficient number of counts [Fig. 8(b)]. Therefore we only tested if a value $\beta = 0°$ was consistent with these data (γ was set equal to 0°). No large disagreement is found, as can be seen in Fig. 8(b).

We thus conclude that the angle between the c axis and the PAS z axis is smaller than 15°. This immediately reveals that the I nucleus does not make equal bonds with its two neighbors. In this case a bond-switching mechanism should occur[14] and the PAS should have the same orientation as for Te in Te with $\beta = 62.5°$. Also, a single bond with one of the Te nearest neighbors has to be excluded, as then the angle should be about 45°. So we must conclude that one of the two Te nearest neighbors has a stronger bond with the I nucleus than the other one. This is in excellent agreement with the analysis of the V_{zz}, η, and δ values given in Ref. 11.

A last remark must be made about the Goldanskii-Karyagin effect in Te. Instead of just summing the $P_k(\theta_i, \phi_i)$ for the three lattice locations, a possible different $f(\theta_i', \phi_i')$ value also has to be taken into account. The angles θ_i' and ϕ_i' are defined relative to the PAS of the mean-square displacement tensor.[1] The resulting intensity ratios are

$$\frac{I_k}{I_l} = \frac{\sum_{i=1,3} P_k(\theta_i, \phi_i) f(\theta_i', \phi_i')}{\sum_{i=1,3} P_l(\theta_i, \phi_i) f(\theta_i', \phi_i')} \quad . \tag{9}$$

However, for $\Theta = 0°$, due to the symmetry of the Te crystal described above, all three $P(\theta_i, \phi_i)$ are the same, as a rotation about the γ-ray direction does not change the θ_i and ϕ_i values. Thus $f(\theta_i', \phi_i')$ drops out from formula (9), and the I_k/I_l values are independent of a possible anisotropic f factor. This cannot be said for the $\Theta = 90°$ direction. However, the consistency of the $\Theta = 90°$ result for ^{125}Te, described above, suggests that the influence of f anisotropy at this angle is very small, consistent with the results of Ref. 1.

VI. CONCLUSION

The experiments with the ^{125m}Te sources, implanted in Te single crystals, demonstrate that nearly all of the implanted ions occupy regular lattice sites, and that the single-crystal character of

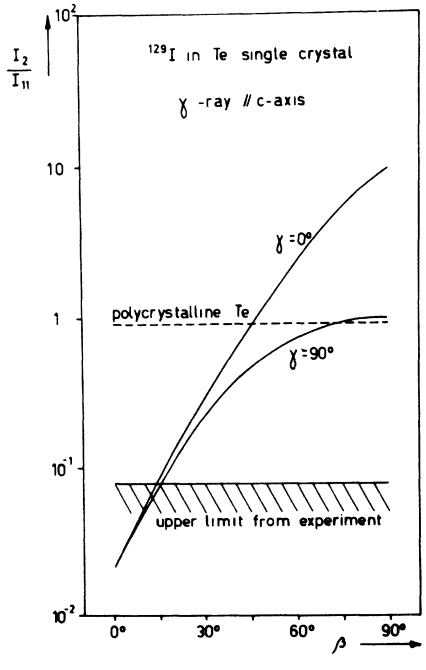

FIG. 9. I_2/I_{11} ratio for ^{129}I in a Te single crystal for γ ray $\parallel$ c axis. The experimental value has been taken from the spectrum in Fig. 8(a). The I_2/I_{11} ratio for polycrystalline Te is also added for comparison.

the source host was not destroyed by implantation damage. We extend these results to the implanted ^{129m}Te sources, where the implantation doses were much lower. In this way, we were able to measure the angle between the crystal c axis and the PAS z axis for an I impurity in a Te single-crystal host, with enough accuracy to use these results in nuclear-orientation experiments at low temperatures, or in perturbed-angular-correlation experiments to measure quadrupole moments. Some preliminary results have already been obtained.

ACKNOWLEDGMENTS

We wish to thank Professor Dr. P. Grosse and Dr. R. Drope (Technische Hochschule, Aachen, Germany) and Dr. D. Fischer (University Würzburg, Germany) for the Te single-crystal samples. We also wish to thank Professor Dr. H. de Waard (University Groningen, The Netherlands) for the CuI absorber. One of the authors (G. L.) wishes to thank the N. F. W. O. for financial support.

APPENDIX

From classical mechanics we know that for the transformation from a (a, b, c)-axis system to a (X_i, Y_i, Z_i)-axis system, described by the Euler angles $(\alpha_i, \beta_i, \gamma_i)$, the following transformation formulas hold:

$$\begin{pmatrix} \sin\theta_i & \cos\phi_i \\ \sin\theta_i & \sin\phi_i \\ \cos\theta_i & \end{pmatrix} = \begin{pmatrix} T^i_{11} & T^i_{12} & T^i_{13} \\ T^i_{21} & T^i_{22} & T^i_{23} \\ T^i_{31} & T^i_{32} & T^i_{33} \end{pmatrix} \times \begin{pmatrix} \sin\Theta & \cos\Phi \\ \sin\Theta & \sin\Phi \\ \cos\Theta & \end{pmatrix}. \tag{A1}$$

The angles θ_i and ϕ_i are expressed relative to the (X_i, Y_i, Z_i)-axis system, and the angles Θ and Φ are expressed relative to the (a, b, c)-axis system (Fig. 6). The elements of the transformation matrix are

$$\begin{aligned}
T^i_{11} &= \cos\gamma\cos\alpha_i - \cos\beta\sin\alpha_i\sin\gamma, \\
T^i_{12} &= \cos\gamma\sin\alpha_i + \cos\beta\cos\alpha_i\sin\gamma, \\
T^i_{13} &= \sin\gamma\sin\beta, \\
T^i_{21} &= -\sin\gamma\cos\alpha_i - \cos\beta\sin\alpha_i\cos\gamma, \\
T^i_{22} &= -\sin\gamma\sin\alpha_i + \cos\beta\cos\alpha_i\cos\gamma, \\
T^i_{23} &= \cos\gamma\sin\beta, \\
T^i_{31} &= \sin\beta\sin\alpha_i, \\
T^i_{32} &= -\sin\beta\cos\alpha_i, \\
T^i_{33} &= \cos\beta.
\end{aligned} \tag{A2}$$

We made use of the fact that $\beta_1 = \beta_2 = \beta_3 = \beta$ and that $\gamma_1 = \gamma_2 = \gamma_3 = \gamma$. Having in mind that $\alpha_1 = \alpha$, $\alpha_2 = \alpha + 120^\circ$, and $\alpha_3 = \alpha + 240^\circ$, we can easily calculate

$$\begin{aligned}
&\sum_i \sin^2\alpha_i = \sum_i \cos^2\alpha_i = \frac{3}{2}, \\
&\sum_i \sin\alpha_i = \sum_i \cos\alpha_i = \sum_i \sin\alpha_i\cos\alpha_i = 0.
\end{aligned} \tag{A3}$$

The first expression we want to transform is $\sum_i \cos^2\theta_i$. Using Eqs. (A1)–(A3), we easily calculate that

$$\begin{aligned}
\sum_i \cos^2\theta_i &= \sum_i (T^i_{31}\sin\Theta\cos\Phi \\
&\quad + T^i_{32}\sin\Theta\sin\Phi + T^i_{33}\cos\Theta)^2 \\
&= \tfrac{3}{2}\sin^2\Theta\sin^2\beta + 3\cos^2\Theta\cos^2\beta.
\end{aligned} \tag{A4}$$

In the same way we calculate that

$$\begin{aligned}
\sum_i \sin^2\theta_i\cos 2\phi_i &= \sum_i (\sin^2\theta_i\cos^2\phi_i - \sin^2\theta_i\sin^2\phi_i) \\
&= (\tfrac{3}{2}\sin^2\Theta\sin^2\beta - 3\cos^2\Theta\sin^2\beta)\cos 2\gamma.
\end{aligned} \tag{A5}$$

---

*Aspirant N. F. W. O.

[1] P. Boolchand, B. L. Robinson, and S. Jha, Phys. Rev. B 2, 3463 (1970).

[2] R. N. Kuzmin, A. A. Opalenko, and V. S. Shpinel, in *Proceedings of the Conference on the Application of the Mössbauer Effect, Tihany*, 1969 (Akademiai Kiado, Budapest, 1971), p. 785.

[3] D. Fischer and P. Grosse, Z. Angew. Phys. 30, 154 (1970).

[4] A. Abragam, *The Principles of Nuclear Magnetism* (Oxford U. P., London, 1961), p. 166.

[5] T. P. Das and E. L. Hahn, in *Solid State Physics*, edited by F. Seitz and D. Turnbull (Academic, New York, 1958), p. 13.

[6] D. W. Hafemeister, G. de Pasquali, and H. de Waard, Phys. Rev. 135, B1089 (1964).

[7] S. V. Karyagin, Sov. Phys. Solid State 8, 1387 (1966).

[8] P. Zory, Phys. Rev. 140, A1401 (1965).

[9] C. E. Violet and R. Booth, Phys. Rev. 144, 225 (1966).

[10] G. K. Shenoy and B. D. Dunlap, Nucl. Instr. Meth. 71, 285 (1969).

[11] M. Pasternak and S. Bukshpan, Phys. Rev. 163, 297 (1967).

[12] J. L. Warren, C. H. W. Jones, and P. Vasudev, J. Phys. Chem. 75, 2867 (1971).

[13] P. Gspan, R. Drope, and P. Grosse, Verhandl. DPG (VI) 5, 286 (1970).

[14] Reference 5, p. 172.